Are heavy rainfall events a major trigger of associated natural hazards along the German rail network?

Sonja Szymczak[1], Frederick Bott[1], Vigile Marie Fabella[1], Katharina Fricke[1]

[1]German Centre for Rail Traffic Research at the Federal Railway Authority, Dresden, 01219, Germany

Correspondence to: Sonja Szymczak (SzymczakS@dzsf.bund.de)

Abstract. Heavy rainfall events and associated natural hazards pose a major threat to rail transport and infrastructure. In this study, the correlation between heavy rainfall events and three associated natural hazards (flood events, gravitational mass movements and tree fall events) were investigated using GIS analyses and random-effects logistic models. The spatio-temporal linkage of a damage database from a German railroad operator and a catalogue on heavy rainfall events from the German Weather Service revealed that almost every part of the German rail network was affected by at least one heavy rainfall event between 2011–2021. Twenty-three percent of the flood events, 14 % of the gravitational mass movements and 2 % of the tree fall events occurred after a heavy rainfall event. The random effects logistic regression models showed that a heavy rainfall event significantly increases the probability of occurrence of a flood (tree fall) by a factor of 34.29 (39.85), respectively, with no significant increase for gravitational mass movements. The heavy rainfall index and the 21-days antecedent precipitation index were determined as characteristics of the heavy rainfall events with the strongest impact on all three natural hazards. The results underline the importance of gaining more precise knowledge about the impact of climate triggers on natural hazard-related disturbances, to make rail transport more resilient.

1 Introduction

Heavy rainfall events are one of the most important triggers for flash floods, which can have catastrophic effects on the affected regions. A prominent recent example is the flood disaster in Western Europe in July 2021 with over 200 fatalities (Kreienkamp et al., 2021). During the period 12 to 15 July 2021 extreme rainfall occurred in Germany and the Benelux countries (Junghänel et al., 2021; Tradowsky et al., 2023). The resulting flash floods caused considerable damage to infrastructure such as houses (Korswagen et al., 2022), communication facilities, roads and railway lines (Szymczak et al., 2022), making the event the deadliest European flooding event in nearly three decades and the costliest on record (Aon, 2021). Damage to critical infrastructures such as power supply and transportation is of particular concern, as efficient infrastructure is important to ensure that affected regions can be reached and supplied with essential goods even in the event of a disaster.

Fortunately, not every heavy rainfall event has such catastrophic effects as the example of July 2021. Nevertheless, at the local level, secondary processes triggered by heavy rainfall, such as landslides, flooding and scouring, can cause considerable economic damage (e.g. Kjekstad and Highland, 2009; Lehmkuhl and Stauch, 2022), especially when transport infrastructure is affected (Klose et al., 2014; Winter et al., 2016). If such events occur along transport networks and disrupt traffic and transport, they are documented by the infrastructure operators. However, these damage databases rarely establish a cause-effect relationship, i.e. there is usually no precise information on which climatic or other parameter triggered the damaging event. This is because *reactive* natural hazard management, i.e. damage repair and rapid restoration of operations, is a higher priority for operators than a detailed documentation of the triggering event. Nevertheless, it should not be neglected that a *proactive* approach, which includes a detailed analysis of the cause-effect relationship between climatic triggers and resulting natural events, contributes significantly to increasing the long-term resilience of transport infrastructure to natural hazards.

Within the framework of proactive natural hazard management (e.g. Mühlhofer et al. 2023), it is possible to identify regions that are particularly at risk, e.g. by developing hazard indication maps, or to determine climatic thresholds for the triggering of certain processes. Particularly in view of the current climate change situation, the management of climatically induced natural hazards is becoming increasingly important in the transportation sector (Koks et al., 2019). Which natural hazards are particularly relevant depends on the region and the mode of transport. In addition to the climatic conditions of the respective region, special features specific to the mode of transport must also be considered. For example, line closures in rail transport have a significantly higher impact than in road transport due to the lower number of alternative routes, and short-term bypasses of rail lines are associated with a higher logistical and personnel effort (Rachoy and Scheikl, 2006). Likewise, the risk of damage is higher and a lower risk tolerance is desirable due to the more complex infrastructure, rail-bound driving, longer braking distance and train length (Mattson and Jenelius, 2015).

In German railroad operations, tree falls, gravitational mass movements and flood events are particularly common natural hazards that cause operational disruptions (Fabella and Szymczak, 2022). These events can be triggered by a variety or a combination of different factors, but heavy rainfall events are possible triggers for all of these processes. This relationship is much clearer for floods and gravitational mass movement processes, while it is not so straightforward for tree falls. There are only a limited number of studies on precipitation induced tree fall events available (e.g. Morimoto et al. 2021), and heavy precipitation events such as the event in July 2021 are often accompanied by wind gusts, so it is difficult to separate clearly what the exact cause of the tree fall event was. However, the influence of soil moisture on the stability and vitality of trees has been proven in various studies (e.g. Hanewinkel et al., 2011; Lucía et al., 2018; Usbeck et al., 2010). As an increase in the intensity of daily and especially sub-daily extremes can be expected in a warmer climate (e.g. Lengfeld et al., 2021; Zeder and Fischer, 2022), special attention of transport operators should be paid to precipitation extremes and associated hazards. In our study, we investigate the relationship between heavy rainfall events and associated natural hazards, such as floods, gravitational mass movements and tree falls, and its impact on the German wide rail network. For this purpose, we first perform a spatio-

temporal linkage of a damage database of DB InfraGO (part of Deutsche Bahn, Germany's largest railroad company) and the catalogue of radar-based heavy rainfall events (CatRaRE) from the German Weather Service (DWD). This analysis should bring any spatial or temporal correlation of the heavy rainfall events and the investigated natural hazards to light. Secondly, we set up random-effects logistic regression models to explore (1) if the probability of the occurrence of natural hazards increase significantly with proximity to a heavy rainfall event and (2) which characteristics of the heavy rainfall events have the strongest impact on the occurrence of the natural hazards.

2 Materials and Methods

2.1 Datasets

In order to carry out the planned analyses, a wide range of data was required, which was collected from various sources. Table 1 provides an overview of all the data used and the most important definitions of how the terms are used in this manuscript. The individual datasets are presented in more detail below.

Table 1: Overview of data used in the study and definition of important terms.

Term	Description
Heavy rainfall event	Warning level W3 (events with 25-40 l/m² in 1 hour or 35-60 l/m² in 6 hours)
Rail / damage events (tree falls, gravitational mass movements, flood events)	Damages recorded by DB InfraGO; resulting from a damage database of DB InfraGO
Damage database	Damage database of DB InfraGO in which the damage events along the railway lines are listed
Natural hazard	In this context: tree falls, gravitational mass movements, flood events
Natural hazard event datasets	Individual datasets of each natural hazard resulting from the damage database of DB InfraGO
Track section (railway)	Defined by the GIS-layer "geo-strecke" provided by DB InfraGO. According to this layer, the German rail netork is divided into 15939 track sections.
Route segment (railway)	A section of the German rail network between two adjacent operating points. The total length of the German rail network owned by DB is 56939 of tracks km, which is divided into 9679 route segments. The segments differ in length between 140 m and 12.7 km with an average length of 3.4 km.
Explanatory control variables	Climatological and hydrometeorological variables related to the investigated natural hazards to check for other relationships in the statistical regression analysis. Variables used in this study are: **daily precipitation**, **daily soil moisture** and **hazard indication map for slope and embankment landslides**.
Observation	Description within the statistical analysis methods for the size of the dataset as a combination of days and route segments. The complete dataset is available for 3987 days (= time-series units) and 9679 route segments, resulting in a total of 38590173 route segment - day combinations. The number of observations used in the succeeding models vary depending on the available time period of the natural hazard event datasets.

2.1.1 CatRaRE of the German Weather Service (DWD)

For Germany, the DWD has developed the so called CatRaRE, a catalogue of heavy rainfall events collected via radar to provide a comprehensive overview on all heavy rainfall events that have occurred in Germany since 2001 (Lengfeld et al., 2021). Each event is described by various parameters such as time, duration, location, mean and maximum precipitation, severity indices as well as meteorological, geographical and demographic information. Strictly speaking, the CatRaRE consists of two catalogues: T5 and W3 (Lengfeld et al., 2022). As no standardized guideline for defining heavy rainfall exists, events for the catalogue were extracted by either (1) their intensity with Warning Level W3 of the official DWD warning levels used as a threshold (W3-catalogue) or (2) their return period taking local conditions into account (T5-catalogue). In the catalogue W3, the lower boundary of warning level 3 is used as a threshold. Warning levels for 1 hour (25 mm), 5 hours (35 mm), 12 hours (40 mm), 24 hours (50 mm), 48 hours (60 mm) and 72 hours (90 m) are defined. We decided to use the W3-catalogue for our analysis as it is more suitable for Germany-wide studies because of the uniform threshold for heavy rainfall events (Lengfeld et al., 2021). As event data from the database of DB InfraGO is only available for the years 2011-2021, only heavy rainfall events from these years were included in our analysis. A total number of 14275 heavy rainfall events occurred in these 11 years. Not all of these events are relevant for our study, since only 7722 events can be spatially intersected with the German rail network. The spatial intersection is achieved considering purely spatial overlap and does not take rainfall runoff conditions into account. Therefore, the resulting map cannot be used as a consideration for recommendations for action because rainfall upstream is not considered. Our intention is to raise awareness that large parts of the German rail network can potentially be affected by heavy rainfall events and that it is therefore necessary to have a closer look on this natural hazard. Throughout the study period, the proportion of events that can be spatially intersected with the rail network remains constant per year at around 50 %. The largest number of events affecting the rail network occurred in 2018 (1160), the lowest in 2012 (454) (Figure 1a). According to Lengfeld et al. (2021), 2018 belongs to the years with the highest number of heavy rainfall events over the entire observation period (2001-2021). The monthly distribution shows a clear seasonal pattern with the majority of events (5682, 73.6 %) occurring in summer (JJA, see Figure 1b). In addition, many heavy rainfall events occurred in May and September, while they were rare during winter. This is consistent with the distribution over the entire period 2001-2021, as May-August are the most eventful months here (Lengfeld et al. 2021). The good resemblance between subplots d and f is quite notable. It is due to the years 2013 and 2016 where very rainy days respectively weeks occurred in May/June, leading to a high number of heavy rainfall events and recorded natural hazards along the German railway network. However, a spatial and temporal intersection of floods and gravitational mass movements could only be observed for a few cases in the dataset so that these processes occurred uncoupled.

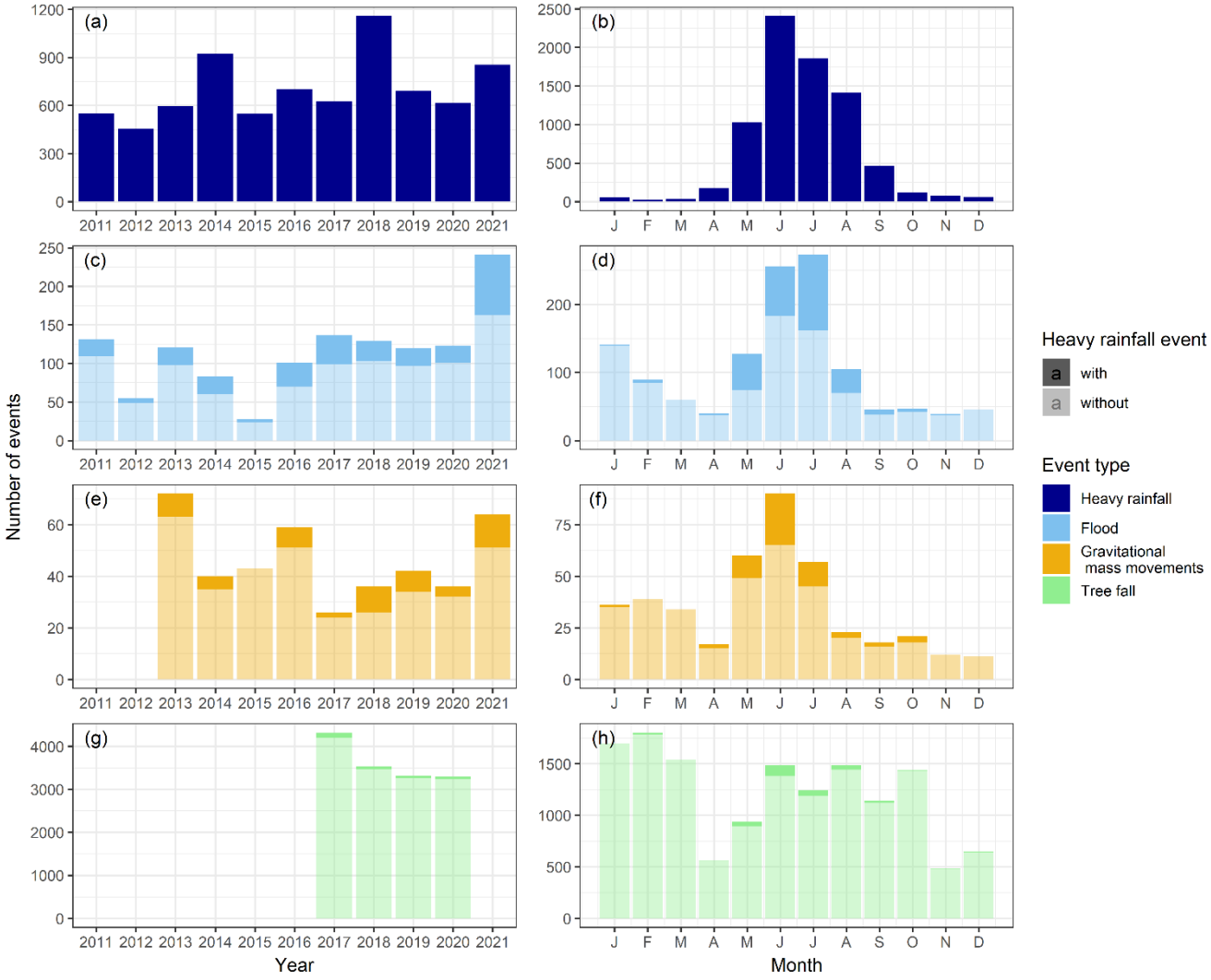

Figure 1: Yearly and monthly distribution of heavy rainfall events (Datasource: CatRaRE) spatially intersected with the German rail network, and gravitational mass movement, flood and tree fall events along the German rail network recorded by the damage database of DB InfraGO. The darker areas of the bars (c – h) include the events where a heavy rainfall event occurred up to two days prior to the event.

The spatial distribution of all heavy rainfall events spatially intersected with the German rail network is shown in Figure 2. The spatial reference used for this analysis were track sections as defined by the GIS-layer "geo-strecke" provided by DB InfraGO, resulting in a total of 15939 track sections. The events are distributed over all regions of Germany with a focus in southern Germany (federal states of Bavaria and Baden-Wuerttemberg). Over the 11-year period, there are very few track sections (437), which were not affected by at least one heavy rainfall event, while most of the pre-alpine railway lines in southern Germany were affected by more than 30 events. However, the "Starkregenindex" SRI of these events is in general

lower. The SRI is based on the return period of the rainfall amount for indices 1-7, where 7 corresponds to a return period of 100 years. Indices 8-12 are based on the rainfall amount compared to a precipitation with a return period of 100 years (Schmitt, 2017; Schmitt et al., 2018). Highest mean SRI-values are recorded in the northern part of Germany, mainly in the federal state of Lower Saxony.

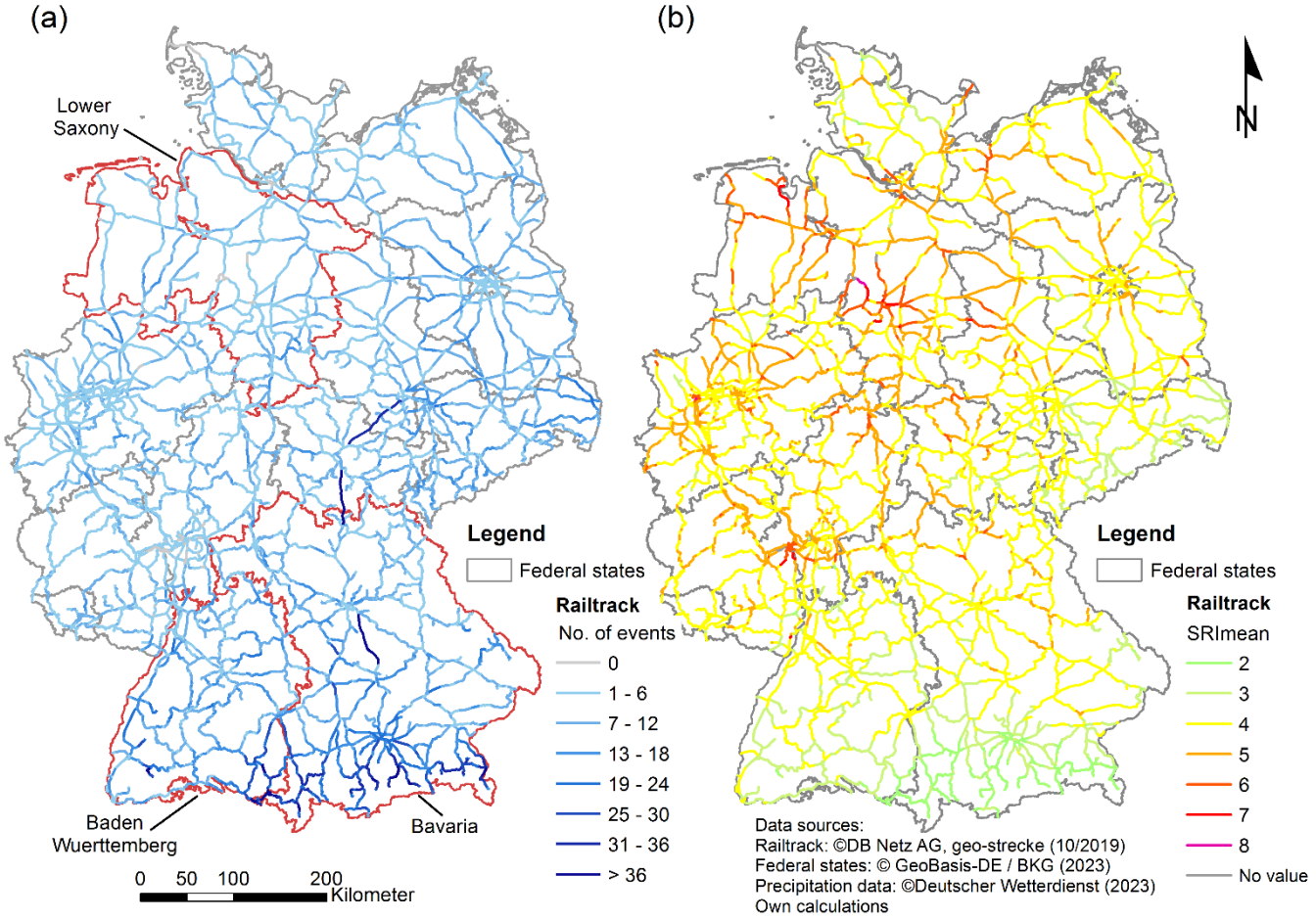

Figure 2: Spatial intersection of heavy rainfall events from the CatRaRE and the German rail network for the time period 2011-2021. a) Number of events per track section. b) Mean SRI-values ("Starkregenindex", for definition refer to Table 1) for all events per track section. The SRI is calculated for every heavy rainfall event and ranges from 0-12. Note that in this figure mean values for several events are shown, limiting the resulting SRI-values to the range 2-8. The location of the federal states mentioned in the manuscript is marked in map (a). Data sources: "geo-strecke" 10/2019 DB InfraGO (rail network), GeoBasis-DE / BKG 2023 (federal states), Deutscher Wetterdienst (heavy rainfall events).

2.1.2 Damage database for the German rail network

The event data of the natural hazards along the German rail network were extracted from a damage database of DB InfraGO. In the database, each disruption along the rail infrastructure is documented with a time stamp, the event location and a short event description. Figure 3 shows an example of each type of natural hazard with an image of the event and the information

contained in the database about the example event. The database is an internal document, and the level of detail of each event depends on the size of the event and the person making the report. This means that for some events, information is also available about which part of the rail system is damaged (e.g. overhead line, switch), but in most cases this remains unclear. In addition, the database is filled by the staff on site along the route, so that, for example, flood events are not differentiated according to their cause (heavy rainfall induced vs. river floods). The date indicates the time of the report, i.e. the time at which the fault was detected. The level of detail also varies between the different processes. For floods and gravitational mass movements, the fields "cause" and "event type" are free text fields, while for tree falls the two options "tree fall" and "branch breakage" can be selected in the field "cluster cause". These fields are not filled in by the staff on site, but by the database managers at DB and thus represent an initial preliminary analysis and classification of events. As this database and data collection is not restricted to natural hazard-specific incidents, the events relevant to this study were filtered using an extended text search with event-specific search terms, such as e.g. branch, tree, landslide or flood, and then checked manually for correctness and double notification. This procedure cannot verify that all events were actually extracted from the database ('completeness') and that there are no false negatives, as the textual descriptions do not follow a fully consistent categorization and thus not all keywords may have been correctly identified. However, the two-step extraction with subsequent manual control of the data ensures the 'correctness' of the data insofar as there are no false positives and no events are contained in the database export due to incorrect assignment. The distribution of false negatives is assumed to be fairly even throughout the study period due to the invariant methods of data collection and filtering.

Figure 3: Examples of recorded events for all three types of natural hazards in the damage database of DB InfraGO. Note that the level of detail is different for the different type of events. For floods and gravitational mass movements, the fields "cause" and "event type" are free text fields, while for tree falls the two options "tree fall" and "branch breakage" can be selected in the field "cluster cause".

In the following, the three resulting sub-databases for flood events, gravitational mass movements and tree falls are briefly described. The flood dataset includes a total of 1269 events for the period 1 January 2011-31 December 2021, which include, but are not further categorized into river floods or local flash floods. The most eventful years were 2021 (241), 2017 (137), 2011 (131) and 2018 (129), while the least eventful years were 2012 (55) and 2015 (28) (Figure 1c). Flood events occurred mainly between May and August with a high concentration in June and July, but also in January (Figure 1d). In contrast, they were rare between September and December. The gravitational mass movement dataset includes a total of 418 events for the period 1 January 2013-31 December 2021, with the most eventful years being 2013 (72), 2021 (64) and 2016 (59), and the least eventful being 2018 and 2020 (36 each) and 2017 (26) (Figure 1e). The monthly distribution showed a concentration of events between May and July and a second, smaller peak between January and March (Figure 1f). The tree fall dataset includes

a total of 14461 events for the period 1 January 2017-16 December 2020. The data for 2021 for tree fall events was different from the recording accuracy compared to the years 2017-2020. In order to avoid misinterpretation due to data inhomogeneity, we decided to exclude the report from 2021 for the tree fall dataset. The most eventful year was 2017 (4319), the least eventful 2020 (3301) (Figure 1g). However, as the last 15 days of the year are missing in 2020, it is also possible that 2019 is the least eventful year (3310). The seasonal distribution of tree fall events is not as pronounced as for the other two processes. Tree fall events occurred mainly between January and March as well as between June and October (Figure 1h).

2.1.3 Explanatory control variables

Additional climatological and hydrometeorological variables related to the investigated natural hazards were used to serve as explanatory control variables (Table 1) and to check for other relationships in the statistical regression analysis. These variables were derived from publicly available datasets provided by the DWD. Daily precipitation values were used from gridded observational datasets of precipitation provided by the HYRAS dataset (Razafimaharo et al., 2020). This dataset is based on precipitation measurements for Germany and its neighboring countries and interpolates them into 1 km x 1 km grids, taking into account topographic and other effects. This dataset was chosen as it has the same resolution as the soil dataset, and is also based on station based observations of precipitation. Daily values of soil moisture were used from a 1 km x 1 km grid developed by the DWD for agrometeorological applications. These values are interpolated from a soil moisture model and soil moisture observations in 60 cm depth under grass at a fixed selection of stations (Löpmeier, 1994). Also included was the hazard indication map for slope and embankment landslides along the German rail tracks provided by the German Centre for Rail Traffic Research at the Federal Railway Authority, which is modeled based on the geology, morphology and land use characteristics of the area surrounding the rail tracks (Kallmeier et al., 2018).

2.2 Methods

2.2.1 Intersection of heavy rainfall events with events from the damage database

The analysis of the spatial and temporal relationship between the heavy rainfall events and damage events along the German rail network was carried out by intersecting the CatRaRE polygon data provided by the DWD and the compiled railway damage database. The polygon area of the CatRaRE data describes the entire area that has been issued as a heavy rainfall event by the DWD. The attributes of the polygon are standardized to the entire polygon. The spatial intersection was carried out using the GIS software ArcMap, version 10.8.1. In ArcMap, the respective damage events floods, gravitational mass movements and tree falls(available as point information) were intersected with the CatRaRE heavy rainfall events (W3-catalogue) between 2011 and 2021 using the tool “Spatial Join”. In the process multiple join features (heavy rainfall events) were assigned to each target feature (damage event (“Join one to many”)). This creates a database in which all spatially overlapping heavy rainfall events are assigned to the damage events. Thus, there are event locations where more than 50 heavy rainfall events from 2011 to 2021 can be found.

Although long-lasting precipitation not categorized as heavy can also trigger floods and can have several impacts on railway infrastructure, the scope of this study is to try to assign flood events to local rainfall extremes occurring in a short time frame before they effect the railway system. So in the context of this study, a heavy rainfall event was only be considered as a trigger for a secondary process if the heavy rainfall event occurs directly or shortly before the damage event. As a heavy rainfall event usually is an event of short duration and high intensity, in general the time lag between trigger and effect is rather short (e.g. shown for shallow landslides by Zêzere et al. (2015) and for landslides during summer by Rupp (2022)). However, heavy rainfall events often occur during weather conditions that lead to clusters of rainfall events, so that the occurrence of several heavy rainfall events in succession can also be a possible cause (e.g. shown for deep-seated landslides by Bevacqua et al. (2021) and for tree fall by Locosselli et al. (2021)). As there is no generally accepted threshold, we have chosen in our study to consider all heavy rainfall events that occurred up to two days before the damage event. This considers possible inaccuracies in the DB damage database, as the date in the damage database represents the time when the event was recorded. This does not necessarily coincide with the actual occurrence of the event, as, for example, events that occur at night are often not recorded until the following day during the first train journey of the day. Furthermore, the selected time period was supported by an analysis of the natural breaks in the dataset. By plotting the days between the occurrence of the damage event and the heavy rainfall event against the number of overlapping events, it is well visible that for all three types of natural hazards up to day 3 a large number of damage events can be linked to a heavy rainfall event that occurred immediately before. From day 4 onwards, this link decreases considerably, so that the heavy rainfall events occurring more than three days before a damage event can no longer be clearly identified as cause for the occurrence of the event. Due to this natural break in the data, the limit value of the difference of three days between the onset of a heavy rainfall event and the damage event was used in the further analyses. The selection of the heavy rainfall events was conducted by temporal intersection using the function “DateDiff” in ArcMap. Since both the damage events and the heavy rainfall events have a day-accurate time stamp, the difference in days between the start of the heavy rainfall event and the occurrence of the damage event could be identified. If several rainfall events occur on the same location within three consecutive days, it is possible that an associated natural hazard process can be attributed to more than one heavy rainfall event. However, this is only the case for a very low number: only one tree fall event, two gravitational mass movements and no flood event are associated with two heavy rainfall events.

2.2.2 Extraction of explanatory control variables

The corresponding values from the explanatory control variables daily precipitation, daily soil moisture and hazard class of landslide risk were extracted from the gridded data at the location and, when applicable, for the date of the event occurrence using the python libraries gdal and ogr.

2.2.3 Statistical analysis and modelling

For the statistical investigation, a panel data analysis as well as a cross-sectional analysis was carried out. The panel data analysis was chosen as statistical method as it allows the analysis of two- or multidimensional panel data by running regression models over chosen dimensions. The method, originating in the econometrics, is used to observe and explore the relationships between observations of heavy rainfall and natural hazard damage events as the relationships may be very complex and the aim is to explore them further. The dimensions of the data collected for panel data analysis are typically covering the temporal and spatial dimension, here they are time and route segment with or without an event/observation as well as additional explanatory variables that take into account the heterogeneity of the studied individuals. The panel dataset has a matrix structure and includes observations and explanatory variables for each individual route segment for each day of the studied time period (Biørn 2017). The individual or in this case the route segment can be observed over a long time period and opposed to time-series and cross-section data, the effects of individual-specific variables as well as time-specific variables can be explored in a panel analysis. A typical panel data regression model is represented by the equation

$$y = \beta_0 + \beta_1 x_{ij} + \beta_2 \varepsilon \quad (1)$$

where y ist the dependent variable, x is the independent variable, β_0, β_1 and β_2 are coefficients and ε is an explanatory control variable, i and j are indices for the dimensions chosen for the analysis (e. g. time and space/individual). The limits of panel data analysis are determined by the data quality and consistency, distortions of measurement errors, short time-series dimensions as well as the relationship between the variables due to potential variable bias and unobserved nuisance variables which are correlated to the observable explanatory variables in the equation (Baltagi 2005; Biørn 2017). In our study, we were interested especially in the probability of which the natural hazard damage events occur in relation to the heavy rainfall events. This was modeled by employing a logit link function, the natural log of the probability that a natural hazard event occurs divided by the probability that it does not occur. Non-linear models are in this case more suitable for modeling binary responses (Wooldridge 2010). To account for the unobserved individual heterogeneity and characteristics (e. g. small scale topography and vegetation) of each route segment, where the damage and heavy rainfall events can occur, a random variable was introduced and a mixed effects logistic regression model with fixed and random effects used for the estimation of the parameters.

A cross-sectional analysis is employing a similar equation and logistic model as the panel analysis, but it aims at exploring the effects of one independent variable upon a dependent variable of interest at a certain point in time. This is done by using econometric methods to effectively hold other factors fixed. This approach is limited when not all control variables are considered and not measured with the same quality (Wooldridge 2010).

2.2.3.1 Panel data analysis

The panel data analysis was conducted to test whether the probability of the occurrence of natural hazards is affected by a heavy rainfall event, and whether the probability increases with proximity in time to a heavy rainfall event. Panel data allows

to consider observations over several points in time, which is crucial for measuring the temporal proximity to a heavy rainfall event at a route segment. Therefore, it is possible to compare the effects of heavy rainfall events that occur at different times before a natural hazard event, e.g. two days before, one day before or at the same day. For the panel data analysis, the dataset was created with route segments as the cross-sectional unit and day as the time-series unit (Table 1). A route segment is defined as a section of the German rail network between two adjacent operating points. An operating point is a railway system defined according to the Railway Construction and Operation Regulations (EBO). Most operating points fall into the categories of stopping point, block point or switch. Operating locations are an important measures and category in the railway industry, serve as the basis for locating events and information along the railway network and were therefore selected. The total length of the German rail network owned by DB is 56939 of tracks km and was divided into 9679 route segments for our dataset. The segments differ in length between 140 m and 12.7 km with an average length of 3.4 km. The length differ because operating points are not evenly distributed over the whole railway network. Route segments were chosen as the cross-sectional unit as it is on the one hand the smallest operational unit used by DB that can represent the complete rail network, and on the other hand, the reported natural hazard events refer to route segments and a corresponding operation point. Additionally, the number of route segments still allows for a tractable data size that does not inflate the calculation times in the statistical analysis, for example compared to taking 5-meter segments across the entire network. The period under consideration were the years between 2011 and 2021 for each route segment, for which it must be tested whether a heavy rainfall event has occurred or not. To calculate 30-days antecedent precipitation (one of the control variables) for each day and route segment, the period started with 1 February 2011, so that the complete dataset is available for 3987 days (= time-series units), resulting in a total of 38590173 route segment - day combinations, hereafter referenced as observations. The number of observations used in the succeeding models vary depending on the available time period of the natural hazard event datasets.

Each observation was spatially intersected with the CatRaRE and the explanatory control variables based on the coordinates of the segment's starting point. Due to the heterogenic shapes and kilometerage of segments, the coordinates of the starting point were regarded as the most accurate and complete information about the localization of the damage events in absence of a more reliable location source. The segment is considered to have been affected by a heavy rainfall event on a given day if a heavy rainfall event from the CatRaRE database has occurred on that day up to a maximum of two days previously. This is then indicated by a binary variable. The flood, gravitational mass movement and tree fall events from the DB damage database were matched to route segments based on their reported route number and kilometer. A natural hazard event can affect more than one route segment. A binary variable was then created for each natural hazard event, which takes the value of one if the respective event was reported on the route segment on that day and zero otherwise.

To test if the probability of the occurrence of natural hazards increase with proximity to a heavy rainfall event, a mixed-effects logistic regression model was used and fixed and random effects added during the research. Taking $p = Pr(Y = 1)$ to be the

probability that a natural hazard event occurs (where Y is either a flood, gravitational mass movement or tree fall), the relationship between this probability p and a heavy rainfall event (HR) was modeled using a logit link function, such that

$$logit(p) = ln\left(\frac{p}{1-p}\right) = \beta_0 + \beta_1\, HR + \boldsymbol{\beta_2'\varepsilon} \tag{2}$$

where ε is a vector of explanatory control variables $\boldsymbol{\varepsilon} = [\boldsymbol{dP}, \boldsymbol{acP}, \boldsymbol{dSM}]$, and β_0, β_1, and $\boldsymbol{\beta_2}$ are the corresponding scalar and vector coefficients. The logit function is simply the natural log of the odds, that is, the natural log of the probability that a natural hazard event occurs (p) divided by the probability that it does not occur ($1-p$).

The basis of interpretation of the model in equation (1) lies in its exponential form, which results in the odds on the left-hand side of the equation:

$$\frac{p}{1-p} = e^{\beta_0} \cdot e^{\beta_1 HR} \cdot e^{\boldsymbol{\beta_2' x}} \tag{3}$$

Taking HR to be a binary variable with a value of one when heavy rainfall occurred in the last three days and zero otherwise, then the exponential form of the coefficient of HR, e^{β_1}, is the odds ratio (OR) between heavy rainfall and no rainfall event, keeping other variables constant:

$$OR = \frac{\left(\frac{p}{1-p} \mid HR = 1\right)}{\left(\frac{p}{1-p} \mid HR = 0\right)} = e^{\beta_1} \tag{4}$$

If indeed a heavy rainfall event increases the probability of a natural hazard event, then the numerator should be greater than the denominator, hence the odds ratio e^{β_1} should exceed one ($e^{\beta_1} > 1$).

To test if the probability of a natural hazard event increases the closer it occurs to days with heavy rainfall events, a second logistic regression model similar to eq. (2) was also estimated,

$$logit(p) = ln\left(\frac{p}{1-p}\right) = \beta_0 + \boldsymbol{\beta_1'\, DHR} + \boldsymbol{\beta_2'\varepsilon} \tag{5}$$

where $\boldsymbol{DHR}$ takes the form of a vector of dummy variables representing the number of days after the heavy rainfall occurred (Table 2),

$$\boldsymbol{DHR} = \begin{bmatrix} d_0 = \text{day of heavy rainfall} \\ d_1 = \text{one day after heavy rainfall} \\ d_2 = \text{two days after heavy rainfall} \end{bmatrix} \tag{6}$$

and $\boldsymbol{\beta_1'} = [\beta_{1,0} \quad \beta_{1,1} \quad \beta_{1,2}]$ are the corresponding parameter coefficients. The assumption that the probability of an event increases the closer it is in time to a heavy rainfall event is confirmed when the odds ratios follow the order $OR_0 > OR_1 > OR_2$, where

$$OR_i = \frac{\left(\frac{p}{1-p} \mid d_i\right)}{\left(\frac{p}{1-p} \mid d_{-1}\right)} = e^{\beta_{1i}}, \qquad i = 0, 1, 2. \tag{7}$$

with d_{-1} as the reference category representing no heavy rainfall in the last three days. The control variables $\boldsymbol{\varepsilon}$ for both regression models in eq. (2) and (5) include other meteorological factors that may affect the incidence of a natural hazard event, such as daily precipitation, 30-day accumulated precipitation, and daily soil moisture (Table 2). Annual and seasonal dummies are also included to account for the fact that the number of natural hazards varies greatly in different years and seasons. The seasonal and annual effects may also lead to characteristics such as varying temperature uncoupled from precipitation, resulting soil infiltration capacity, vitality of the vegetation, foliage coverage, onset of the vegetation period, distribution of storms without heavy rainfall etc. that were not captured by the input data. Therefore, the binary dummy variables were added.

Table 2: Abbreviations and descriptions of the characteristics of heavy rainfall events in the CatRaRE and control variables from other dataset that were used for the panel data analysis in this study.

	Abbr.		Variable	Description
Dummy variables	HR		0 to 2 days from heavy rainfall event	Binary dummy variable that describes whether the damage event took place between the day of a heavy rainfall event or up to two days after
	DHR	d_0	- day of heavy rainfall	Binary dummy variable that describes whether the damage event took place on the day of a heavy rainfall event
		d_1	- 1 day after heavy rainfall	Binary dummy variable that describes whether the damage event took place one day after a heavy rainfall event
		d_2	- 2 days after heavy rainfall	Binary dummy variable that describes whether the damage event took place two days after a heavy rainfall event
Control variables	dP		Precipitation at route segment [mm]	Daily precipitation on the day of the damage event from the 1 km x 1 km HYRAS dataset
	acP		Accumulated precipitation at route segment, 30 days [mm]	30-days antecedent precipitation calculated based on daily precipitation from the 1 km x 1 km HYRAS dataset
	dSM		Daily soil moisture at route segment [% nFK]	Daily soil moisture on the day of the damage event from DWD soil moisture 1 km x 1 km grid for agrometeoroligcal applications

Given the panel structure of the data, observations from the same route segment may be correlated with each other. To overcome this issue, models in eq. (2) and (5) were extended to include a random variable μ_r representing the unobserved individual heterogeneity of each route segment r,

$$logit(p_{rt}) = ln\left(\frac{p_{rt}}{1-p_{rt}}\right) = \beta_0 + \beta_1\, HR_{rt} + \boldsymbol{\beta_2'}\boldsymbol{\varepsilon_{rt}} + \mu_r \tag{8a}$$

$$logit(p_{rt}) = ln\left(\frac{p_{rt}}{1-p_{rt}}\right) = \beta_0 + \boldsymbol{\beta_1'}\,\boldsymbol{DHR_{rt}} + \boldsymbol{\beta_2'}\boldsymbol{\varepsilon_{rt}} + \mu_r \tag{8b}$$

where the subscript $t = 1, \ldots, 4011$ identifies the days in the sample. The parameters of the mixed-effects models are estimated using maximum likelihood. Given that all the explanatory variables in the models (HR_{rt}, $\boldsymbol{DHR_{rt}}$ and $\boldsymbol{\varepsilon_{rt}}$) are exogenous meteorological factors, the individual-specific component μ_i is expected to be uncorrelated with all the regressors in the

models. It was necessary to introduce this variable as during the development and testing of the panel analysis not all route segment characteristics could be presented by the hazard class and topographic information. We suspect that the input data resolution is in some cases not sufficient to characterize the route segments in detail, may it be due to the small scale location of the tracks on a slightly elevated dam, the actual exposition, and other mitigating factors such as drainage ditches etc. The variable μ_r therefore represents the random effect for route segment r, which is typically assumed to be independently and identically distributed across route segments following a normal distribution $N(0, \sigma_\mu^2)$. Higher variance σ_μ^2 indicates a higher correlation between two observations within the same route segment.

To test whether there are interaction effects between the control variables and heavy rainfall events, the following interaction terms are added to eq. (8a): daily precipitation $dP * HR_{rt}$, 30-day accumulated precipitation $acP * HR_{rt}$, and daily soil moisture $dSM * HR_{rt}$.

$$logit(p_{rt}) = ln\left(\frac{p_{rt}}{1-p_{rt}}\right) = \beta_0 + \beta_1 HR_{rt} + \boldsymbol{\beta_2'\varepsilon_{rt}} + \beta_3 dP_{rt} HR_{rt} + \beta_4 acP_{rt} HR_{rt} + \beta_5 dSM_{rt} HR_{rt} + \mu_r \quad (9a)$$

$$logit(p_{rt}) = ln\left(\frac{p_{rt}}{1-p_{rt}}\right) = \beta_0 + \boldsymbol{\beta_1' DHR_{rt}} + \boldsymbol{\beta_2'\varepsilon_{rt}} + \beta_3 dP_{rt} HR_{rt} + \beta_4 acP_{rt} HR_{rt} + \beta_5 dSM_{rt} HR_{rt} + \mu_r \quad (9b)$$

As a certain time lag between the occurrence of a heavy rainfall event and a natural hazard could be observed, these additional interaction terms were introduced to account for possible preexisting soil water calculated solely based on the precipitation or also considering evapotranspiration. The various parameters were all investigated despite carrying information about very similar triggers for damage events to give more insight into the magnitude of the relationship between measurements or indicators and different damage events. A larger problem may be the different scales of the variable units when compared against each other. Equations (9a) and (9b) were then used to calculate the mixed-effects logit model and exponentiated coefficients for each natural hazard event type separately; the results are presented in Table 2 and 3 as well as in Figure 4.

2.2.3.1 Cross-sectional analysis

The cross-sectional analysis was conducted to examine which characteristics of a heavy rainfall event have the strongest effect on natural hazard occurrence. In cross-sectional analyses, each observation is only considered at a single point in time. Since heavy rainfall events differ considerably in intensity, duration and other features, the cross-sectional analysis was used to test which of these characteristics influence the occurrence of a natural hazard event. The cross-sectional dataset contains only those route segments hit by at least one heavy rainfall event between 2011 and 2021. This resulted in a total number of 9339 route segments, of which 8589 were affected more than once during the eleven-year period, on average about five times. Each combination of route segment and heavy rainfall event is considered as a separate observation in the cross-sectional dataset. From the panel dataset, it can be determined whether a natural hazard event occurred during and up to two days after a heavy

rainfall event on this specific route segment. For each heavy rainfall event, several characteristics are available in the CatRaRE, of which a selection was used in this study (Table 3).

Table 3: Abbreviations and descriptions of the characteristics of heavy rainfall events in the CatRaRE that were used for the cross-sectional analysis in this study.

Abbreviation	Description
H	Duration [h] of the heavy rainfall event
RRmean	Mean precipitation [mm] of all RADKLIM pixels within the event zone
SRImean	Mean of the heavy rainfall index (in German "Starkregenindex"): An index based on the return period of the rainfall amount for indices 1-7, where 7 corresponds to a return period of 100 years. Indices 8-12 are based on the rainfall amount compared to a precipitation with a return period of 100 years. Mean of all RADKLIM-pixels within the event zone (Range [0,12])
V3_AVG	Mean of the 21-days antecedent precipitation index within the event zone
ETA	A measure of the extremity of the heavy rain event as a function of the return period as well as affected area of an event
VSGL_GRAD	Mean degree of sealing [%]: Percentage of sealed area including road infrastructure within the event zone
STRM_AVG	Mean elevation [m] above sea level within the event zone
TPI_AVG	Mean of the Topographic Position Index, 2 km circular neighborhood [m], in the event zone within Germany. The index is calculated as the difference between the height of a cell in the DTM and the average height of all neighbouring cells in the sliding window around this cell. It can approximate the topographical wind exposure of mountain and valley locations.

Considering a similar logistic model as in the panel analysis, the relationship between the characteristics of the heavy rainfall events and the probability (p_e) that a natural hazard occurs in observation of an event e, is assumed to take the form

$$logit(p_e) = ln\left(\frac{p_e}{1-p_e}\right) = \beta_0 + \boldsymbol{\beta_1'}\boldsymbol{Z_e} + \boldsymbol{\beta_2'}\boldsymbol{\varepsilon_e} \quad (10)$$

where $\boldsymbol{Z_e} = [z_{e,1} \quad \cdots \quad z_{e,8}]$ is a vector of the eight aforementioned characteristics in Table 3 and $\boldsymbol{\beta'_1} = [\beta_{1,1} \quad \cdots \quad \beta_{1,8}]$ are the corresponding parameter coefficients. Since the variables in $\boldsymbol{Z_e}$ are continuous, the interpretation of the odds ratios is based on a one-unit increase in the value of the variable of interest:

$$OR_j = \frac{\left(\frac{p}{1-p}\,|\,z_j + 1\right)}{\left(\frac{p}{1-p}\,|\,z_j\right)} = e^{\beta_{1j}}, \qquad j = 1, 2, \ldots, 8. \quad (11)$$

The maximum likelihood method was used to estimate the parameters in this cross-sectional logistic model in eq. (10) for all three hazard event datasets separately. The results are presented in Table 6.

3 Results

3.1 Spatial intersection of heavy rainfall events and natural hazards

Of the 1269 flooding events, a total of 296 (23 %) can be spatially and temporally linked to a heavy rainfall event. A total of 184 (62 %) of the flooding events linked to heavy rainfall occur in June and July with July being the front-runner (111 events) (Figure 1d). There are also a large number of coupled events in May and August, while the number is below ten events in the other months. The lowest number is in March and December (zero each) and January and November (two each). The distribution over the years varies between four (2015) and 78 (2021) events. Besides 2021, the most frequent overlaps occur in 2016 and 2017. Of the 418 gravitational mass movement events, a total of 59 events (14 %) can be spatially and temporally linked to a heavy rainfall event, most of them (48 or 81 %) between May and July (Figure 1f). The distribution among the years varies between zero (2011, 2012, 2015) and 13 (2021) events. Besides 2021, the most frequent intersections occur in 2013, 2016, 2018 and 2019. Of the 14461 tree fall events, a total of 312 (2 %) events can be spatially and temporally linked to a heavy rainfall event. A total of 163 of the tree falls (35 %) linked to heavy rainfall occur in June and July with June being the front-runner (108 events) (Figure 1h). There are also a large number of coupled events in May (40) and August (46), followed by September (21) and February (20). The lowest number occurs in November (1) and January (2). The distribution across years varies between 57 (2019) and 118 (2017) events.

A comparative analysis of all three natural hazards shows that in all three processes mainly the hazard events in summer are coupled with heavy rainfall events (Figure 4). In contrast, the hazard events in winter are predominantly not coupled with heavy rainfall events. The figure shows all three hazard processes together, however, the distribution looks similar for each process when viewed individually.

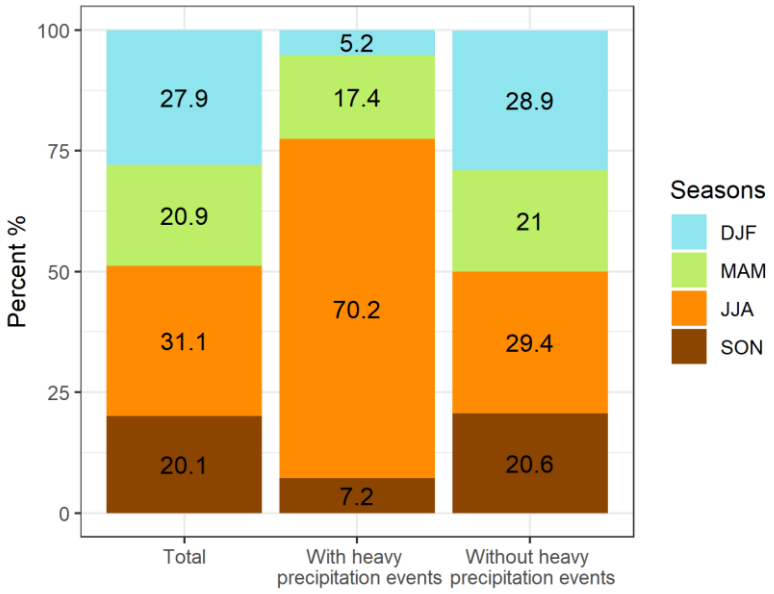

Figure 4: Seasonal distribution of natural hazard events reported for the German rail network coupled with and without heavy rainfall events. All three natural hazard processes are shown together in the figure, as the distribution looks similar for each process when viewed individually.

3.2 Influence of heavy rainfall events on the occurrence of natural hazard events

Table 4 provides the estimated odds ratios of the mixed-effects logit models in eq. (3) for the three different natural hazard events. The dataset of the entire period contains a total of 38590173 observations, but this number is lower for gravitational mass movements and tree falls because of the shorter available time period of the natural hazard event datasets. To evaluate model performance, several model criteria were calculated and presented in Table 4. Several values are provided to evaluate the goodness of fit for the models: The log likelihood is a function of the sample size, the higher the value of the log likelihood the better. The comparison between model calculated on different datasets is associated with uncertainty, a limited comparability can be achieved by scaling the log likelihood with the number of observations used. The rho value shows the contribution of the random effect to the total variance. The Akaike's information criteria (AIC) is an estimator of the prediction error and calculated based on the number of independent variables and the log-likelihood estimate. The lower the AIC, the better a model fits the data it was generated from. AIC calculated with different datasets can be evaluated considering the size of the data sets but offer only a limited comparability.

Table 4: Results of the random effects logit model for incidence of a natural hazard after a heavy rainfall event. The number of observations is lower for gravitational mass movements and tree fall events as for floods because of the shorter time period under consideration.

	Dependent variable		
	Flood	Gravitational Mass Movement	Tree Fall
Heavy rainfall, last 3 days=1	**34.29****	3.812	**39.85*****
	(41.71)	(11.26)	(29.91)
Precipitation at route segment [mm]	**1.079*****	**1.052*****	**1.069*****
	(0.00360)	(0.00691)	(0.00117)
Accumulated precipitation at route segment, 30 days [mm]	**1.010*****	**1.014*****	**1.003*****
	(0.000843)	(0.00128)	(0.000293)
Daily soil moisture at route segment [% nFK]	**0.944*****	0.957	**0.931*****
	(0.0138)	(0.0233)	(0.00316)
Observations	38590173	31795515	14141019
Number of route segments	9679	9679	9679
Log likelihood	-10645.3	-4322.7	-87853.1
Rho	0.430	0.531	0.375
AIC	2338.6	8689.5	175740.3

Exponentiated coefficients (odds ratios); Standard errors in parentheses; All models include season and year controls, and interaction terms.

* $p < 0.05$, ** $p < 0.01$, *** $p < 0.001$

According to the results, a flood event is on average 34 times more likely to occur if a heavy rainfall event occurred on the day of or up to two days before the flood than if no heavy rainfall event occurred. Tree fall events are on average even more likely to occur (almost 40 times). Both results are statistically significant at 0.01. In contrast, there is no evidence of a statistically significant difference between the odds of a gravitational mass movement with and without heavy rainfall. To provide insight in the temporal relationship between heavy rainfall events and resulting natural hazards, the random effects logit models were also calculated with the vector dummy variables in equation (8) representing the number of days after the heavy rainfall occurred (Table 5). Regarding the time lag, the probability of flood events is highest when the heavy rainfall event occurred on the same day as the flood event, and decreases with increasing temporal distance. All values are statistically significant. This means that compared to a situation with no occurring heavy rainfall, a heavy rainfall event is close to 12 times more likely to cause a flood on the same day, while 10 times more likely to cause a flood the day after, and almost 5 times more likely to cause a flood after two days. The magnitude of the log likelihood and the AIC values convey that the model for tree fall events has the lowest quality and highest prediction error while the model for floods and gravitational mass movements both have a higher model quality and lower prediction error. Despite the lower number of observations of events available for the gravitational mass movements, the model and chosen variables describe the relationship between gravitational mass movements and heavy rainfall events accurately. In the case of tree fall events the actually by a magnitude higher number of data points available for the calculation does not lead to a better model fit, which may indicate that additional factors not covered in the chosen variable set do influence the occurrence of tree falls. According to the values of rho for the three models, the contribution of random effects to the total variance is highest for gravitational mass movements. Here the route segment characteristics not described by the control variables are contributing more to the dependent variable than in other events.

Table 5: Results of the random effects logit model for incidence of a natural hazard with different numbers of days after a heavy rainfall event.

	Dependent variable		
	Flood	Gravitational Mass Movement	Tree Fall
Days from heavy rainfall event			
- day of heavy rainfall	**11.93*****	**3.691*****	**0.296*****
	(1.925)	(1.402)	(0.0482)
- 1 day after heavy rainfall	**9.886*****	**10.91*****	**2.411*****
	(1.650)	(2.861)	(0.302)
- 2 days after heavy rainfall	**4.718*****	1.131	0.920
	(1.070)	(0.817)	(0.186)
Precipitation at route segment [mm]	**1.023*****	**1.022*****	**1.054*****
	(0.00211)	(0.00464)	(0.00150)
Accumulated precipitation at route segment, 30 days [mm]	**1.011*****	**1.014*****	**1.004*****
	(0.000781)	(0.00126)	(0.000294)
Daily soil moisture at route segment [% nFK]	**1.023*****	**1.011***	**1.017*****
	(0.00295)	(0.00457)	(0.000820)
Observations	38590173	31795515	14141019
Number of route segments	9679	9679	9679
Log likelihood	-10789.5	-4343.9	-88528.8
rho	0.430	0.535	0.376
AIC	21621.0	8725.7	177085.6

Exponentiated coefficients (odds ratios); Standard errors in parentheses; All models include season and year controls.
* $p < 0.05$, ** $p < 0.01$, *** $p < 0.001$

For gravitational mass movement and tree fall events, the relationship is weaker than for flood events and even insignificant for heavy rainfall events occurring two days before the natural hazard event. Interestingly, the highest odds ratios can be observed for gravitational mass movements when the heavy rainfall event occurred one day before the natural hazard. This means that a gravitational mass movement is close to eleven times more likely compared to a situation with no heavy rainfall, and more than two times more likely compared to when heavy rainfall occurs on the same day. After two days, the probability of a gravitational mass movement is no longer different from a situation with no heavy rainfall. For tree fall events, the odds ratio on the day of a heavy rainfall is 0.296 and statistically significant, meaning that the probability of a tree fall event occurring on the same day as a heavy rainfall is less than a third that of a situation when no heavy rainfall occurs. In contrast, one day after a heavy rainfall event, a tree fall event is 2.4 times more likely to occur than in days with no heavy rainfall. After two days, the odds ratio is no longer statistically different from one. Although heavy rainfall events directly affect only 2 % of tree fall events, they can increase the probability of their occurrence. However, this increase is only a relative increase compared to the case without an associated heavy rainfall event. As both events (heavy rainfall as well as tree fall) are very rare events in relation to the route network and the time period in days, it must be considered that the probability of an event occurring is still low. The goodness of fit of the models, the expected residual error, the contribution of the random effects to the variance and subsequent conclusions seem to be comparable to the results in Table 5.

In Tables 4 and 5, the odds ratios of the control variables precipitation and 30-day accumulated precipitation are statistically significant and slightly greater than one. The estimates are relatively smaller in magnitude compared to that of the heavy rainfall variables, which is to be expected from the continuous nature of the precipitation variables. In Table 5, for example, a one-millimeter increase in precipitation increases the odds of a flood event by a factor of 1.023, a mass movement event by a factor of 1.022 and a tree fall event by a factor of 1.054. On the other hand, a one-millimeter increase in 30-day accumulated precipitation increases the odds of a flood event by a factor of 1.011, a mass movement event by a factor of 1.014 and a tree fall event by a factor of 1.004. These estimates do not vary considerably across the two models in equation (3) (Tables 4 and 5). In contrast, the results for daily soil moisture is ambiguous and not robust to changes in the specification of the heavy rainfall variable. In Table 4, the estimates of the odds ratios for daily soil moisture are below zero, meaning a one-percentage point increase in soil moisture leads to lower odds of all three natural hazards. In Table 5, the opposite is the case, the estimated odds ratios are greater than one, meaning the odds of a natural hazard event is higher with a one-percentage point increase in daily soil moisture. This could indicate that daily soil moisture has a non-linear effect on the occurrence of the three natural hazards. The analysis not broken down by individual days (Table 4) shows that a higher soil moisture has a slightly negative effect on the probability, while the analysis broken down by days shows a slight positive influence (Table 5). As both results are significant, this could either be a false correlation or an indication of non-linear effects, the latter is supported by Figure 5.

The influence of the three control variables precipitation, accumulated precipitation of 30 days and daily soil moisture on the relationship between heavy rainfall and the occurrence of a natural hazard event is analyzed using the results of the interaction terms and is depicted graphically in Figure 5. The analysis used the equation 8a) with the coefficients calculated for the different natural hazards. For the available range of the control variables, the probability calculated with the three different models is shown. The modelled probability of the occurrence is compared for the case that no heavy rainfall event and the case that a heavy rainfall event occurred over a broad range of control variable values on the same day of the natural hazard event. The curves and the probability for the situation “with heavy rainfall event” are above the curves “without heavy rainfall event” for all three types of natural hazards and all three control variables, indicating that the probability of a natural hazard occurring is always higher with a preceding heavy rainfall event. However, the curves have different shapes. In several subplots, both curves show a slight increase and the distance between them remains about the same (a), d), h)). This means that the difference in the probability of occurrence is independent of the amount of precipitation. In the case of b) and e), the distance becomes greater at higher values, i.e. the higher the amount of accumulated precipitation, the more a heavy rainfall event increases the probability of occurrence of a flood or gravitational mass movement. For c) and i), the curve “with heavy rainfall event” has a U-shape. Thus, the probability of a natural hazard occurring during a heavy rainfall event is higher when the soil moisture takes on extreme values than when it takes on average values. In the case of tree fall, this is particularly the case for low soil moisture values, and in the case of floods for high soil moisture values. The arc shape in f) indicates that the probability of occurrence is highest at medium soil moisture values. In the case of g), both curves slightly converge at high values, i.e. the higher the amount of precipitation, the less a heavy rainfall event increases the probability of occurrence of a tree fall event.

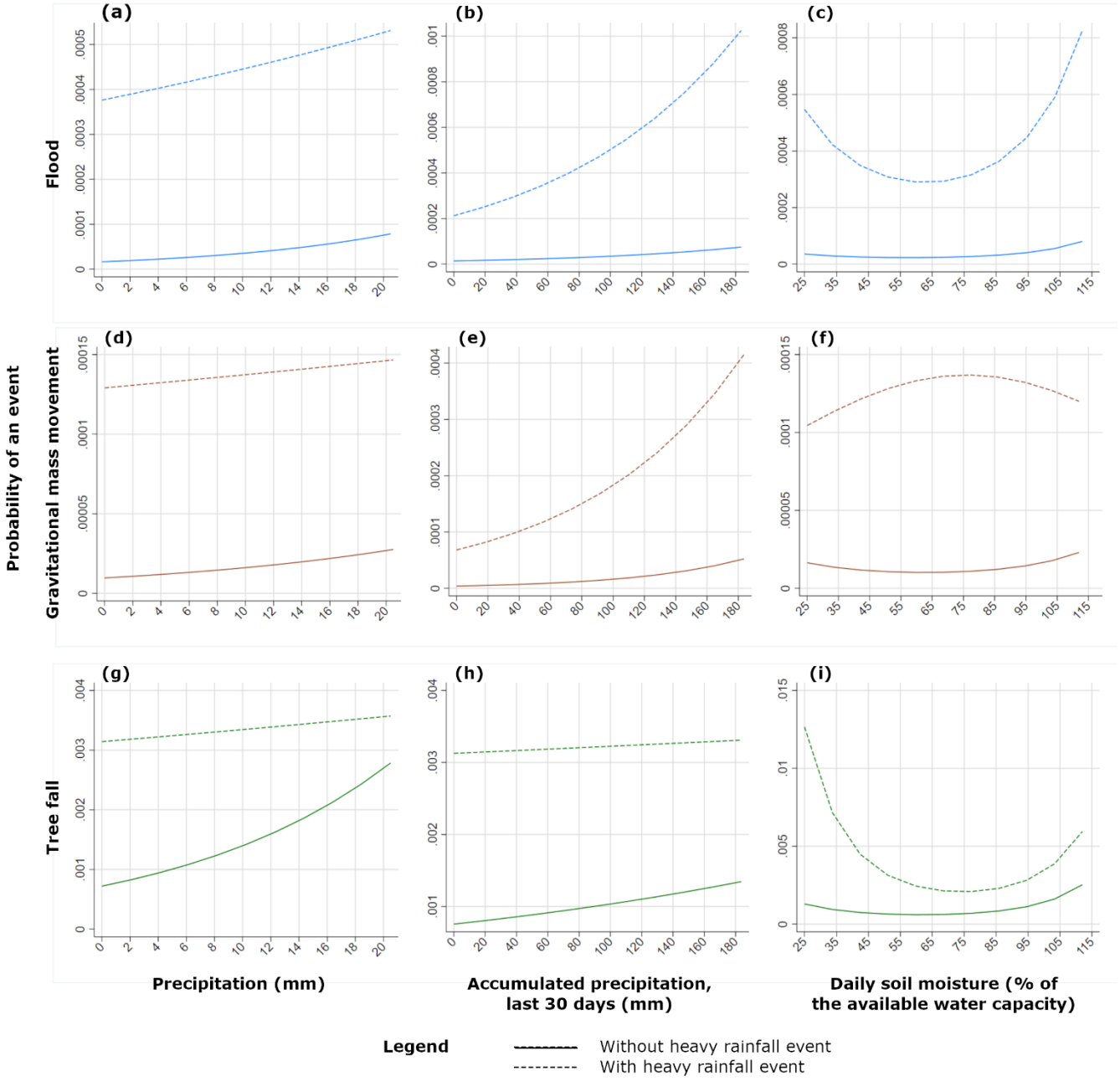

490 **Figure 5: The influence of the control variables precipitation, accumulated precipitation and soil moisture on the probability of occurrence of flood, gravitational mass movement and tree fall events. Each box compares the probability of occurrence for the two cases "without heavy rainfall event" and "with heavy rainfall event".**

3.3 Characteristics of heavy rainfall events and their influence on the occurrence of natural hazards

The previous section has shown that the occurrence of heavy rainfall events has a statistically significant influence on the occurrence of natural hazards, particularly flood and tree fall events. However, as heavy rainfall events can be described with various parameters, the aim of the cross-sectional analysis was to investigate which characteristics of the heavy rainfall events affect the probability of natural hazard events and how these effects differ across the three processes. Table 6 presents the resulting odds ratios of the estimated logistic regression model of the cross-sectional analysis when the parameter in question is increased by one unit. The duration of the heavy rainfall event and the mean precipitation throughout the area affected by the heavy rainfall event does not seem to have a significant effect on the probability of a natural hazard. However, the heavy rainfall index (SRImean) does significantly increase the probability of all three natural hazards. When the index increases by one unit, the odds increase by a factor of 1.577 (floods), 1.716 (gravitational mass movements) and 1.389 (tree falls), respectively. The table also reveals the significant effect of 21-days antecedent precipitation index (API) on all three types of natural hazards. A one-millimeter increase in the API increases the odds by a factor of 1.05.5 (flood), 1.075 (gravitational mass movements) and 1.025 (tree fall), respectively. When normalized with the number of the observation, the magnitude of the log likelihood and the AIC values convey that the model for tree fall events has the lowest quality and highest prediction error while the model for gravitational mass movements has the highest model quality and lowest prediction error, while the model for floods falls in between.

Table 6: Results of the cross-sectional logit model on the components of heavy rainfall events and their effect on the odd ratios of the probability of occurrence of flood, gravitational mass movement and tree fall events. Note that the number of observations is reduced compared to Table 2 and 3, as the cross-sectional dataset contains only those route segments hit by at least one heavy rainfall event between 2011 and 2021.

	Dependent Variable		
	Flood	Gravitational Mass Movement	Tree Fall
Duration of heavy rain [h]	1.000	1.002	1.000
	(0.002)	(0.005)	(0.002)
Mean precipitation [mm] of all pixels within the event zone (RRmean)	1.015	1.007	1.002
	(0.009)	(0.021)	(0.010)
Mean heavy precipitation index of all pixels within the event zone (SRImean)	**1.577*****	**1.716*****	**1.389*****
	(0.103)	(0.242)	(0.089)
21-days antecedent precipitation index - Mean within the event zone (V3_AVG)	**1.055*****	**1.075*****	**1.025****
	(0.008)	(0.017)	(0.009)
Extremity, mean throughout event duration (Eta)	1.003	1.002	0.997
	(0.002)	(0.005)	(0.002)
Degree of soil sealing [%] within the event area, mean (VSGL_GRAD)	0.978	0.984	**0.936*****
	(0.013)	(0.021)	(0.014)
Mean elevation [m] above sea level in the event zone (STRM_AVG)	1.000	**0.998****	0.999
	(0.0003)	(0.001)	(0.0004)

Topographic Position Index [m] - Mean within event zone (TPI_AVG)	1.049	1.016	0.982
	(0.037)	(0.105)	(0.026)
Constant	0.0001***	0.00001	0.0002
	(0.0001)	(0.001)	(0.009)
Observations	47605	41646	24132
Log Likelihood	-1566.481	-348.888	-1326.230
Akaike Inf. Crit.	3180.963	741.777	2688.459

Exponentiated coefficients (odds ratios); Standard errors in parentheses
* $p < 0.05$, ** $p < 0.01$, *** $p < 0.001$

The geographical characteristics within the heavy rainfall event zone that shows a significant influence on the occurrence of natural hazards are the degree of soil sealing and elevation. The degree of soil sealing has a negative effect on tree fall events and one percent of increased soil sealing reduces the odds by a factor of 0.936 (statistically significant at 0.1). Similarly, the mean elevation within the heavy rainfall area reduces the odds of gravitational mass movement events by a factor of 0.998.

4 Discussion

4.1 Heavy rainfall events and associated natural hazards

The heavy rainfall event in July 2021 was an exceptional event in terms of intensity and spatial extent (Tradowsky et al., 2023). Such devasting flash floods are therefore not to be expected with every heavy rainfall event occurring in Germany. Nevertheless, less intense heavy rainfall events are not a rare phenomenon in Germany; they can occur anywhere and are seasonally concentrated in the summer months. About 50 % of all heavy rainfall events between 2011 and 2021 can be spatially intersected with the German rail network, and almost the entire rail network has been affected by a heavy rainfall event at least once during this 11-year period. Heavy rainfall events and associated natural hazards can therefore potentially affect the entire German rail network. However, vulnerability varies greatly from region to region and is determined, for example, by the route of the line in relation to the topography (Braud et al., 2020). Routes that follow valley courses or cross low mountain ranges are particularly prone to associated processes such as gravitational mass movements and local flooding. In order to make rail transport more resilient to heavy rainfall, it is important to gain a more detailed knowledge about cause-effect relationships between heavy rainfall events and the disruptions they trigger.

Often it is not the heavy rainfall event itself that cause damage to transport infrastructure, but processes that are triggered by them. Relationships between heavy rainfall events as a triggering factor for further processes such as flooding (Bernet et al., 2019; Wake, 2013) and various types of gravitational mass movements (Araújo et al., 2022; Huggel et al., 2012; Kirschbaum et al., 2022; Tichavský et al., 2019) have already been established in several studies. Similarly, the regression models in our study show that heavy rainfall events can in the two days following the event significantly increase the occurrence probability of flood by a factor of 34.29 and tree fall events by a factor of 39.85 (see Table 4). The probability of flood events decreases

the more time passed after the heavy rainfall event, while the probability of tree fall events peaks the day after a heavy rainfall event (Table 5). The increased probability of gravitational mass movement events is only statistically significant the day of and the day after a heavy rainfall event, but is also strongly correlated to precipitation and accumulated precipitation (Tables 4 and 5). It is therefore important not to consider the occurrence of different natural hazards individually, but to establish connections between the triggering factor and the resulting hazard, for example, by looking at gravitational mass movements triggered by flooding. On a conceptual level, establishing climate impact chains (e.g. UBA, 2021) or application of compound-hazard approaches (e.g. Zscheischler et al., 2020) are recommended.

About a quarter of all flood events could be coupled with a heavy rainfall event, and for gravitational mass movements it was as much as 17 % (Figure 1). The proportion of tree fall events connected to heavy rainfall events is very low, which could be due to the fact that storms and strong winds are considered the main trigger for this type of event (e.g. Bíl et al., 2017; Gardiner et al., 2010). Additionally, wind gusts (Gardiner et al., 2024) or flooding (Lucía et al. 2018) can cause tree fall events. A large proportion of the tree fall disturbances recorded in the DB damage database have been caused by a few large autumn and winter storms, such as Friederike in January 2018 (286 reports) or Sabine in February 2020 (513 reports), which were characterized by prolonged precipitation rather than heavy rainfall events. The influence of heavy rainfall on increasing the risk of tree fall has hardly been studied so far. Morimoto et al. (2021) found that heavy rainfall connected to typhoons increases the probability of disturbances in forest stands. Even if a spatial and temporal overlap of a heavy rainfall with an event from the damage database could be determined, it must be emphasized once again at this point that the heavy rainfall event can only be considered as a possible cause for the event and the actual causal trigger cannot be derived from the DB damage database. With our study, we would like to show how damage data from infrastructure operators can be merged with climate data from weather services to establish a potential relationship. This step represents an important contribution in terms of proactive natural hazard management to identify the route sections that are particularly affected by certain climatic parameters and associated processes. Furthermore, this information can be used to prioritize adaptation needs.

The parameters Heavy Rainfall Index (SRI) and Antecedent Precipitation Index (V3) are the properties of the heavy rainfall events that most strongly influence the occurrence of all three natural hazard processes considered (Table 6, Figure 5). Thus, it is a combination of the pre-moisture conditions of the soil due to previous rainfall events and the occurrence of a heavy rainfall event, which most clearly promotes the occurrence of the processes. This is in concordance with, for example, findings from Saito et al. (2014) and Rupp (2022). Saito et al. (2014) tested for rainfall-triggered landslides whether the volume of landslides can be predicted directly from rainfall totals, intensity and duration. They suggest that increasing rainfall totals enhance landslide activity up to a certain threshold beyond which the effect does not apply. The increase is also supported by our study (Fig 4 b) and e)), but a threshold was not reached in our dataset, possibly due to the lower number of mass movement events in our dataset compared to Saito et al. (2014). Rupp (2022) analyzed the triggering factors for landslides with seasonal resolution. The antecedent precipitation is of great importance for the occurrence of landslides all year round, but especially

in winter. Locosselli et al. (2021) found a similar seasonal variability for the climate drivers for tree falls among urban trees in Brazil. During the wet season, temperature has a direct influence on tree fall, while precipitation and wind gusts can have lagged effects. The CatRaRE of DWD provides antecedent precipitation indexes for two time periods, 21-days and 30-days. These are the most common models for modelling pre-moisture. As the natural hazards investigated in our study were examined in relation to heavy rainfall events occurring shortly before, the 21-day antecedent is considered a useful parameter, as it reflects the medium-term conditions at the respective locations well and therefore an influence of this on the occurrence of sudden natural hazards was assumed and proven in the analyses.

The influence of soil moisture on the three types of natural hazards as shown in Figure 5 makes sense in terms of physics. The probability of a flood is exactly the opposite to the soil infiltration capacity depending on the soil moisture content. Water infiltration is low when the soil is especially dry, and the pores are closed as well as when they are overfull. The probability of a flood is therefore higher if soil moisture content is low or high. The influence of soil moisture on gravitational mass movements is not significant (Fig. 5f), but a tendency is shown that high water infiltration may lead to slope destabilization and therefore simplify the triggering of a gravitational mass movement. In the case of tree falls, soil moisture have an influence on tree vitality. At very low soil moisture, trees suffer from drought stress, and tree vitality significantly influences the risk of tree fall (Honkaniemi et al., 2017; Krisans et al., 2020). Similar, trees are more unstable in the case of high soil moisture, which can easier trigger tree fall events.

No information on the magnitude of the hazard events can be obtained from the damage database. The duration of the disturbance, which is given for flood and tree fall events only, shows that for floods 33 % of the events have a disturbance duration of more than one day, for tree falls only 2 % (Fabella and Szymczak, 2021). From the rather short disruption durations, it can be deduced that most of the events must be smaller, as it is not possible to resume operations after a short time in the case of a larger event. In the case of smaller events, the small-scale climate conditions, as represented for example by SRI and V3, are most important. Hence, no significant correlations could be observed with the larger-scale parameters such as mean precipitation, mean topographic position index and mean daily soil moisture. The role of the parameter degree of soil sealing (VSGL) on tree falls could be explained by the fact that areas with a high degree of sealing tend to have fewer trees along the track that can potentially cause disturbances, while more rural and less sealed areas have more trees and therefore also an increased risk of tree fall events.

4.2 Data availability and quality

While the data quality of the CatRaRE is very high, it is difficult to validate the quality and completeness of the DB damage database. Therefore, it must be taken into account that the relatively low numbers of damage reports that could be linked to a heavy rainfall event are only minimum values due to the different background intended or original purpose of the data collections. While the DWD is responsible for meeting the meteorological needs of all economic and social sectors in Germany,

the DB damage database is an internal product. The main task of a railroad operator is to ensure safe railroad operations. The focus is not on the detailed recording of the damage event with exact process allocation, cause, etc., but rather on enabling a quick repair and ensuring the resumption of railroad operations. The database is not filled by experts, but by the staff on site along the route. It is therefore possible, that technical terms are not always used correctly and e.g. flood events are not differentiated according to their cause. Additionally, an event is only recorded if it disrupts the railway operations, so there may occur heavy rainfall events or river floods that are not captured in the dataset. However, disruptions caused by natural hazards account for a substantial proportion of disruption events overall. In 2018, for example, weather-related disruptions were the second most frequent cause of cancellations according to DB data (Deutscher Bundestag, 2019). As climate change advances, it can be assumed that the number and extent of disruptive events is more likely to increase rather than decrease in the future, unless targeted countermeasures are taken. It is therefore essential to adapt rail transport and rail infrastructure to climate change. However, this requires reliable data on past damage events in order to guarantee a statistically robust consequence-based risk assessment and the targeted development of measures for action in the future. We therefore recommend improving the documentation requirements for the various modes of transport in order to create a reliable damage database in the long-term. This should also include a subdivision of natural hazard events according to the underlying processes. For instance, river floods are typically caused by (longer) precipitation runoff in larger areas of the river watershed, while local flash floods are caused by the immediate runoff of concentrated, intense heavy rainfall events (Penna et al., 2013). A river flood can be produced by upstream rainfall rather than by local rainfall, and this rainfall may not reach local extreme thresholds and may not intersect with the location where a damage on the railroad infrastructure is observed. These events therefore could not be detected with the method presented in this study, thus explaining partly the result that only a quarter of the flood events could be linked to extreme rainfall events. As the information in the database on each event are limited, it is unfortunately not possible to evaluate which proportion of the events relate to river flooding. Additionally, gravitational mass movements encompasses a broad range of different processes, all of which have very different triggering factors and recurrence times. However, no clear process assignment can be derived from the event data along the rail network. We therefore recommend for the future to classify gravitational mass movements in the database according to their volume and type of transported materials, transportation processes and triggers, as e.g. heavy rainfall events typically trigger shallow landslides, while accumulated rainfall contributes more to deeper landslides (Zêzere et al., 2015).

4.3 Future development of heavy rainfall events and associated hazards

In Western and Central Europe, extreme rainfall has already increased in frequency and will, with high confidence, continue to increase further with climate change (Seneviratne et al., 2021). However, modelling current and future trends in heavy rainfall events on a regional scale is a challenging task. Rybka et al. (2022) used a convection-permitting regional climate model to estimate return levels dependent on the rainfall duration and return period for Germany. They found a 30 % mean increase in intensity for daily rainfall extremes for the end of the 21st century assuming a high-end emission scenario, but the model shows no further increase in intensity for sub-daily heavy rainfall estimates. Although the exact rate is a subject of

debate, it can be assumed that with rising temperatures more water vapor can potentially be retained in the atmosphere, thus increasing the potential for the occurrence of heavy rainfall events (Lengfeld et al., 2021; Zeder and Fischer, 2020). Several studies using observational data (e.g. Westra et al., 2013) or modeling experiments (e.g. O'Gorman, 2015) tested successfully the hypothesis that the intensity of daily extreme rainfall follows roughly the Clausis-Clapeyron relationship, e.g. an increase of roughly 7 % per °C ambient temperature (Allen and Ingram, 2002; Trenberth, 1999). An increase in daily (e.g. Westra et al., 2014; Fischer and Knutti, 2015) and sub-daily precipitation (e.g. Lenderink and Meijgaard, 2008; Guerreiro et al., 2018) extremes is already observed in several studies over many regions. Especially in the summer months, with a combination of long dry periods interrupted by single heavy precipitation periods, it can be assumed that these heavy rainfall events can lead to an increase of associated processes, e.g. landslides (Tichavský et al., 2019).

The timespan of the DB damage database it too short to analyze trends in the occurrence of the three types of natural hazards. Access to high quality data on past natural hazard-related disruptions in the transport sector is a major limitation and one of the reasons while there are only few scientific studies available on this issue (e.g. Braud et al., 2020; Donnini et al., 2017; Fabella and Szymczak, 2021; Gardiner et al. (2024)). However, quantifying the impact of natural hazards on the transport sector is of great importance, especially with regard to climate change. A global study by Koks et al. (2019) shows that already today about 27 % of all road and rail assets are exposed to at least one natural hazard. Climate change has a significant impact on forest stability (Seidl et al., 2017), and the frequency and magnitude of several natural hazards are likely to increase with ongoing climate change, as shown for gravitational mass movements (e.g. Chiang and Chang, 2011; Gariano and Guzzetti, 2016) or flash floods (e.g. Kundzewicz et al., 2013). It is therefore very likely that disturbances along transport routes due to natural hazards will occur more frequently in the future.

5 Conclusions

Due to the heavy rainfall event in July 2021 and the resulting flash floods and damage, awareness of vulnerability to this natural hazard has increased significantly and, among other things, a large number of research activities has been initiated. As the rail infrastructure was particularly hard hit, we contribute to raising awareness in the rail sector and in the transport sector in general with our study. We were able to show that heavy rainfall events have a significant influence on the occurrence of associated natural hazards. Furthermore, we demonstrate an approach to link climate data with damage data of a transport mode in order to establish a correlational interdependence. This can also be applied to other climate impacts and other modes of transport and represents an important component in the context of proactive natural hazard management.

Data availability

The CatRaRE data used for this study are available at https://www.dwd.de/DE/leistungen/catrare/catrare.html.

Author contributions

Conceptualisation: SS, FB, VF and KF; methodology: SS, FB, VF and KF; software: FB, VF and KF; data analysis and interpretation: SS, FB, VF and KF; writing – original draft preparation: SS; writing – review and editing: SS, FB, VF and KF; visualisation: FB, VF and KF. All authors have read and agreed to the published version of the manuscript.

Competing interests

The contact author has declared that none of the authors has any competing interests.

Acknowledgments

The authors thanks DB InfraGO for providing data from the damage database.

References

Allen, M.R. and Ingram, W.J.: Constraints on future changes in climate and the hydrologic cycle, Nature, 419 (6903), 224-232, 2002.

Aon: Global Catastrophe Recap: July 2021, Aon-Report, London, 19 p., 2021.

Araújo, J.R., Ramos, A.M., Soares, P.M.M., Melo, R., Oliveira, S.C., and Trigo, R.M.: Impact of extreme rainfall events on landslide activity in Portugal under climate change scenarios, Landslides, 19, 2279-2293, doi: 10.1007/s10346-022-01895-7, 2022.

Baltagi, B.H.: Econometric Analysis of Panel Data, John Wiley & Sons, Chichester, England, third edition, 317 p, 2005.

Bernet, D.B., Trefalt, S., Martius, O., Weingartner, R., Mosimann, M., Röhtlisberger, V., and Zischg, A.P.: Characterizing precipitation events leading to surface water flood damage over large regions of complex terrain, Environ. Res. Lett., 14, 064010, doi: 10.1088/1748-9326/ab127c, 2019.

Bevacqua, E., De Michele, C., Manning, C., Couasnon, A., Ribeiro, A.F.S., Ramos, A.M., Vignotto, E., Bastos, A., Blesić, S., Durante, F., and 10 further co-autohors: Guidelines for Studying Diverse Types of Compound Weather and Climate Events, Earth's Future, 9, e2021EF002340, doi: 10.1029/2021EF002340, 2021.

Bíl, M., Andrášik, R., Nezval, V., and Bílová, M.: Identifying locations along railway networks with the highest tree fall hazard, Applied Geography, 87, 45-53, doi: 10.1016/j.apgeog.2017.07.012, 2017.

Biørn, E.: Econometrics of Panel Data – Methods and Applications, Oxford University Press, Oxford, England, 42 p, 2017.

Braud, I., Lagadec, L.-R., Moulin, L., Chazelle, B., and Beil, P.: A method to use proxy data of runoff-related impacts for the evaluation of a model mapping intense storm runoff hazard: application to the railway context, Natural Hazards and Earth System Sciences, 20, 947-966, doi: 10.5194/nhess-20-947-2020, 2020.

Chiang, S.-H. and Chang, K.-T.: The potential impact of climate change on typhoon-triggered landslides in Taiwan, 2010-2099, Geomorphology, 133 (3-4), 143-151, doi: 10.1016/j.geomorph.2010.12.028, 2011.

Deutscher Bundestag: Beantwortung der kleinen Anfragen vom 11. März 2019, Deutscher Bundestag, Drucksache 19/8434, 2019.

Donnini, M., Napolitano, E., Salvati, P., Ardizzone, F., Bucci, F., Fiorucci, F., Santangelo, M., Cardinali, M., and Guzzetti, F.: Impact of event landslides on road networks: a statistical analysis of two Italian case studies, Landslides, 14, 1521-1535, doi: 10.1007/s10346-017-0829-4, 2017.

Fabella, V.M. and Szymczak, S.: Resilience of Railway Transport to Four Types of Natural Hazards: An Analysis of Daily Train Volumes, Infrastructures, 6(12), 174, doi: 10.3390/infrastructures6120174, 2021.

Fischer, E.M. and Knutti, R.: Anthropogenic contribution to global occurrence of heavy-precipitation and high-temperature extremes, Nat. Clim. Chang., 5 (6), 560-564, 2015.

Gardiner, B., Blennow, K., Carnus, J.-M., Fleischer, P., Ingemarson, F., Landmann, G., Lindner, M., Marzano, M., Nicoll, B., Orazio, C., Peyron, J.-L., Reviron, M.-P., Schelhaas, M.-J., Schuck, A., Spielmann, M., and Usbeck, T. (Eds.): Destructive storms in European forests: past and forthcoming impacts, European Forest Institute, Joensuu, Finland, 138 pp, https://doi.org/10.13140/RG.2.1.1420.4006, 2010.

Gardiner, B., Lorenz, R., Hanewinkel, M., Schmitz, B., Bott, F., Szymczak, S., Frick, A., and Ulbrich, U.: Predicting the Risk of Tree Fall onto Railway Lines, Forest Ecology and Management, 553, 121614, https://doi.org/10.1016/j.foreco.2023.121614, 2024.

Gariano, S.L. and Guzzetti, F.: Landslides in a changing climate, Earth-Science Reviews, 162, 227-252, doi: 10.1016/j.earscierev.2016.08.011, 2016.

Guerreiro, S.B., Fowler, H.J., Barbero, R., Westra, S., Lenderink, G., Blenkinsop, S., Lewis, E., and Li, X.F.: Detection of continental-scale intensification of hourly rainfall extremes, Nat. Clim. Chang., 8 (9), 803-807, 2018.

Hanewinkel, M., Hummel, S., and Albrecht, A.: Assessing natural hazards in forestry for risk management: a review, Eur J Forest Res, 130, 329-351, doi: 10.1007/s10342-010-0392-1, 2011.

Hokaniemi, J., Lehtonen, M., Väisänen, H., and Peltola, H.: Effects of wood decay by *heterobasidion annosum* on the vulnerability of Norway spruce stands to wind damage: A mechanistic modelling approach, Can. J. For. Res., 47, 777-787, doi: 10.1139/cjfr-2016-0505, 2017.

Huggel, C., Clague, J.J., and Korup, O.: Is climate change responsible for changing landslide activity in high mountains?, Earth Surf. Process. Landforms, 37 (1), 77-91, 2012.

Junghänel, T., Bissolli, P., Daßler, J., Fleckenstein, R., Imbery, F., Janssen, W., Kaspar, F., Lengfeld, K., Leppelt, T., Rauthe, M., Rauthe-Schöch, A., Rocek, M., Walawender, E., and Weigl, E.: Hydro-klimatische Einordnung der Stark- und Dauerniederschläge in Teilen Deutschlands im Zusammenhang mit dem Tiefdruckgebiet Bernd, vom 12. bis 19. Juli 2021, Report, Deutscher Wetterdienst, 2021.

Kallmeier, E., Knobloch, A., and Hertwig, T.: Erstellung einer ingenieurgeologischen Gefahrenhinweiskarte zu Hang- und Böschungsrutschungen entlang des deutschen Schienennetzes, EBA-Forschungsbericht 2018-13, doi: 10.48755/dzsf.210024.01, 2018.

Kirschbaum, D., Kapnick, S.B., Stanley, T., and Pascale, S.: Changes in Extreme Precipitation and Landslides Over High Mountain Asia, Geophysical Research Letters, 47, e2019GL085347, doi: 10.1029/2019GL085347, 2022.

Kjekstad, O. and Highland, L.: Economic and Social Impacts of Landslides, in: Landslides – Disaster Risk Reduction, edited by: Sassa, K. and Canuti, P., Springer, Berlin, Heidelberg, 573-587, 2009.

Klose, M., Damm, B., and Terhorst, B.: Landslide cost modeling for transportation infrastructures: a methodological approach, Landslides, doi: 10.1007/s10346-014-0481-1, 2014.

Koks, E., Rozenberg, J., Zorn, C., Tariverdi, M., Vousdoukas, M., Fraser, S.A., Hall, J.W., and Hallegatte, S.: A global multi-hazard risk analysis of road and railway infrastructure assets, Nat. Commun., 10, 2677, https://doi.org/10.1038/s41467-019-10442-3, 2019.

Korswagen, P., Harish, S., Oetjen, J., and Wüthrich, D.: Post-flood field survey of the Ahr Valley (Germany) – Building damages and hydraulic aspects, TU Delft Report, 69 p., doi: 10.4233/uuid:3cadf772-facd-4e3a-8b1a-cee978562ff1, 2022.

Kreienkamp, F., Philip, S.Y., Tradowsky, J.S., Kew, S.F., Lorenz, P., Arrighi, J., Belleflamme, A., Bettmann, T., Caluwaerts, S., Chan, S.C., and 29 further co-authors: Rapid attribution of heavy rainfall events leading to the severe flooding in Western Europe during July 2021, World Weather. Attrib., 54 p, available online: https://www.worldweatherattribution.org/wp-content/uploads/Scientific-report-Western-Europe-floods-2021-attribution.pdf, 2021

Krisans, O., Matisons, R., Rust, S., Burnevica, N., Bruna, L., Elferts, D., Kalvane, L., and Jansons, A., Presence of root rot reduces stability of Norway spruce (*Picea abies*): Results of static pulling tests in Latvia, Forests, 11, 1-8, doi: 10.3390/F11040416, 2020.

Kundzewicz, Z.W., Kanae, Shinjiro, Seneviratne, S.I., Handmer, J., Nicholls, N., Peduzzi, P., Mechler, R., Bouwer, L.M., Arnell, N., Mach, K., Muir-Wood, R., Brakenridge, G.R., Kron, W., Benito, G., Honda, Y., Takahashi, K., and Sherstyukov, B.: Flood risk and climate change: global and regional perspectives, Hydrological Sciences Journal, 59 (1), 1-28, doi: 10.1080/02626667.2013.857411, 2013.

Lehmkuhl, F. and Stauch, G.: Anthropogenic influence of open pit mining on river floods, an example of the Blessem flood 2021, Geomorphology, 421, 108522, doi: 10.1016/j.geomorph.2022.108522, 2022.

Lenderink, G. and van Meijgaard, E.: Linking increases in hourly precipitation extremes to atmospheric temperature and moisture changes, Environ. Res. Lett., 5, 1-9, 2008.

Lengfeld, K., Kirstetter, P.-E., Fowler, H.J., Yu, J., Becker, A., Flamig, Z., and Gourley, J.: Use of radar data for characterizing extreme precipitation at fine scales and short durations, Environ. Res. Lett., 15, doi: 10.1088/1748-9326/ab98b4, 2020.

Lengfeld, K., Walawender, E., Winterrath, T., and Becker, A.: CatRaRE: A Catalogue of radar-based heavy rainfall events in Germany derived from 20 years of data, Meteorologische Zeitschrift, 30 (6), 469-487, doi: 10.1127/metz/2021/1088, 2021.

Lengfeld, K., Walawender, E., Winterrath, T., Weigl, E., and Becker, A.: Heavy precipitation events version 2022.01 exceeding DWD warning level 3 for severe weather based on RADKLIM-RW version 2017.002, doi: 10.5676/DWD/CatRaRE_W3_Eta_v2022.01, 2022.

Locosselli, G.M., Miyahara, A.A.L., Cerqueira, P., and Buckeridge, M.S.: Climate drivers of tree fall on the streets of Sao Pauli, Brazil, Trees, 35, 1807-1815, doi: 10.1007/s00468-021-02145-4, 2021.

Löpmeier, F.-J.: Berechnung der Bodenfeuchte und Verdunstung mittels agrarmeteorologischer Modelle, Zeitschrift für Bewässerungswirtschaft, 29, 157-167, 1994.

Lucía, A., Schwientek, M., Eberle, J., and Zarfl, C.: Planform changes and large wood dynamics in two torrents during a severe flash flood in Braunsbach, Germany 2016, Science of the Total Environment, 640-641, 315-326, doi: 10.1016/j.scitotenv.2018.05.186, 2018.

Mattson, L.-G. and Jenelius, E.: Vulnerability and resilience of transport systems—A discussion of recent research, Transp. Res. Part A Policy Pract., 81, 16-34, 2015.

Morimoto, J., Aiba, M., Furukawa, F., Mishima, Y., Yoshimura, N., Nayak, S., Takemi, T., Haga, C., Matsui, T., and Nakamura, F.: Risk assessment of forest disturbance by typhoons with heavy precipitation in northern Japan, Forest Ecology and Management, 479, 118521, doi: 10.1016/j.foreco.2020.118521, 2021.

Mühlhofer, E., Koks, E.E., Kropf, C.M., Sansavini, G., and Bresch, D.N.: A generalized natural hazard risk modelling framework for infrastructure failure cascades, Reliability Engineering and System Safety, 234, 109194, doi: 10.1016/j.ress.2023.109194, 2023.

O'Gorman, P.A.: Precipitation Extremes Under Climate Change, Curr. Clim. Chang. Reports, 1, 49-59, 2015.

Penna, D., Borga, M., and Zoccatelli, D.: Analysis of flash-flood runoff response, with examples from major European events, in: Shroder, J. (Editor in Chief), Marston, R.A., Stoffel, M. (Eds.), Treatise on Geomorphology, edited by: Shroder, J., Marston, R.A., and Stoffel, M., Academic Press, San Diego, USA, 95-104, doi: 10.1016/B978-0-12-818234-5.60052-4, 2013.

Rachoy, C. and Scheikl, M.: Anthropogenic caused mass movements and their impact on railway lines in Austria, in: Disaster Mitigation of Debris Flows, Slope Failures and Landslides, edited by: Marui, H. and Mikos, M., Universal Academy Press, Tokyo, Japan, 639-643, 2006.

Razafimaharo, C., Krähenmann, S., Höpp, S., Rauthe, M., and Deutschländer, T.: New high-resolution gridded dataset of daily mean, minimum, and maximum temperature and relative humidity for Central Europe (HYRAS), Theoretical and Applied Climatology, 142, 1531-1553, doi: 10.1007/s00704-020-03388-w, 2020.

Rupp, S.: Effect of the antecedent precipitation on the occurrence of landslides: Examples from the Central Uplands in Germany, Zeitschrift für Geomorphologie, 64 (1), 1-16, doi: 10.1127/zfg/2022/0751, 2022.

Rybka, H., Haller, M., Brienen, S., Brauch, J., Früh, B., Junghänel, T., Lengfeld, K., Walter, A., and Winterrath, T.: Convection-permitting climate simulations with COSMO-CLM for Germany: Analysis of present and future daily and sub-daily extreme precipitation, Meterologische Zeitschrift (Contrib. Atm. Sci.), 32 (2), 91-111, doi: 10.1127/metz/2022/1147, 2022.

Saito, H., Korup, O., Uchida, T., Hayashi, S., and Oguchi, T.: Rainfall conditions, typhoon frequency, and contemporary landslide erosion in Japan, Geology, 42 (11), 999-1002, doi: 10.1130/G35680.1, 2014.

Schmitt, T.G.: Ortsbezogene Regenhöhen im Starkrenindexkonzept SRI12 zur Risikokommunikation in der kommunalen Überflutungsvorsorge, KA Korrespondenz Abwasser, Abfall, 64(4), 294-300, doi: 10.3242/kae2017.04.001, 2017.

Schmitt, T.G., Krüger, M., Pfister, A., Becker, M., Mudersbach, C., Fuchs, L., Hoppe, H., and Lakes, I.: Einheitliches Konzept zur Bewertung von Starkregenereignissen mittels Starkregenindex, KA Korrespondenz Abwasser, Abfall, 65(2), 113-120, doi: 10.3242/kae2018.02.002, 2018.

Seidl, R., Thom, D., Kautz, M., Martin-Benito, D., Peltoniemi, M., Vacchiano, G., Wild, J., Ascoli, D., Petr, M., Honkaniemi, J., Lexer, M.J., Trotsiuk, V. Mairota, P., Scoboda, M., Fabrika, M., Nagel, T.A., and Reyer, C.P.O.: Forest disturbances under climate change, Nature climate change, 7, 395-402, doi: 10.1038/NCLIATE3303., 2017

Seneviratne, S.I., Zhang, X., Adnan, M., Badi, W., Dereczynski, C., Di Luca, A., Ghosh, S., Iskandar, I., Kossin, J., Lewis, S., Otto, F., Pinto, I., Satoh, M., Vicente-Serrano, S., Wehner, M., and Zhou, B.: Climate Change 2021: The Physical Science Basis. Contribution of Working Group I to the Sixth Assessment Report of the Intergovernmental Panel on Climate Change, Chapter Weather and Climate Extreme Events in a Changing Climate, Cambridge, Cambridge University Press, 1513-1766, 2021.

Szymczak, S., Backendorf, F., Bott, F., Fricke, K., Junghänel, T., and Walawender, E.: Impacts of Heavy and Persistent Precipitation on Railroad Infrastucture in July 2021: A Case Study from the Ahr Valley, Rhineland-Palatinate, Germany, Atmosphere, 13(7), doi: 10.3390/atmos13071118, 2022.

Tichavský, R., Ballesteros-Cánovas, J.A., Šilhán, K., Tolasz, R., and Stoffel, M.: Dry Spells and Extreme Precipitation are The Main Trigger of Landslides in Central Europe, Scientific Reports, 9 (14560), doi: 10.1038/s41598-019-51148-2, 2019.

Tradowsky, J.S., Philip, S.Y., Kreienkamp, F., Kew, S.F., Lorenz, P., Arrighi, J., Bettmann, T., Caluwaerts, S., Chan, S.C., De Cruz, L., and 27 further co-authors: Attribution of the heavy rainfall events leading to severe flooding in Western Europe during July 2021, Climate Change, 176 (90), doi: 10.1007/s10584-023-03502-7, 2023.

Trenberth, K.E.: Conceptual framework for changes of extremes of the hydrological cycles with climate change, Clim. Change, 42, 317-339, 1999.

Umweltbundesamt (UBA): Climate Impact and Risk Assessment 2021 for Germany – Summary. Umweltbundesamt, Dessau-Roßlau, 111 p, 2021.

Usbeck, T., Wohlgemuth, T., Dobbertin, M., Pfister, C., Bürgi, A., and Rebetez, M.: Increaseing storm damage to forests in Switzerland from 1858 to 2007, Agricultural and Forest Meteorology, 150, 47-55, doi: 10.1016/j.agrformet.2009.08.010, 2010.

Wake, B.: Flooding costs, Nat. Clim. Chang., 3 (9), 778, 2013.

Westra, S., Alexander, L.V., and Zwiers, F.W.: Global increasing trends in annual maximum daily precipitation, J. Clim., 26 (11), 3904-3918, 2013.

Westra, S., Fowler, H.J., Evans, J.P., Alexander, L.V., Berg, P., Johnson, F., Kendon, E.J., Lenderink, G., and Roberts, N.M.: Future changes to the intensity and frequency of short-duration extreme rainfall, Rev. Geophys., 52 (3), 522-555, 2014.

Winter, M.G., Shearer, B., Palmer, D., Peeling, D., Harmer, C., and Sharpe, J.: The Economic Impact of Landslides and Floods on the Road Network, Procedia Engineering, 143, 1425-1434, doi: 10.1016/j.proeng.2016.06.168, 2016.

Wooldridge, J.M.: Econometric Analysis of Cross Section and Panel Data, The MIT Press, Cambridge, Massachusetts, second edition, 741 p, 2010.

Zeder, J. and Fischer, E.M.: Observed extreme precipitation trends and scaling in Central Europe, Weather and Climate Extremes, doi: 10.1016/j.wace.2020.100266, 2020.

Zêzere, J.L., Vaz, T., Pereira, S., Oliveira, S.C., Marques, R., and Garcia, R.A.C.: Rainfall thresholds for landslide activity in Portugal: A state of the art, Environmental Earth Sciences, 73(6), 2917-2936, doi: 10.1007/s12665-014-3672-0, 2015.

Zscheischler, J. and Fischer, E.M.: The record-breaking compound hot and dry 2018 growing season in Germany, Wea. Climate Extremes, 29, 100270, doi: 10.1016/j.wace.2020.100270, 2020.

Zscheischler, J., Martius, O., Westra, S., Bevacqua, E., Raymond, C., Horton, R.M., van den Hurk, B., AghaKouchak, A., Jézéquel, A., Mahecha, M.D., Maraun, D., Ramos, A.M., Ridder, N.N., Thiery, W., and Vignotto, E.: A typology of compound weather and climate events, Nature Reviews Earth & Environment, 1, 333-348, doi: 10.1038/s43017-020-0060-z, 2020.